USGS
science for a changing world

Prepared for the National Aeronautics and Space Administration

Geological Map of the Nepenthes Planum Region, Mars

By James A. Skinner, Jr., and Kenneth L. Tanaka

Pamphlet to accompany

Scientific Investigations Map 3389

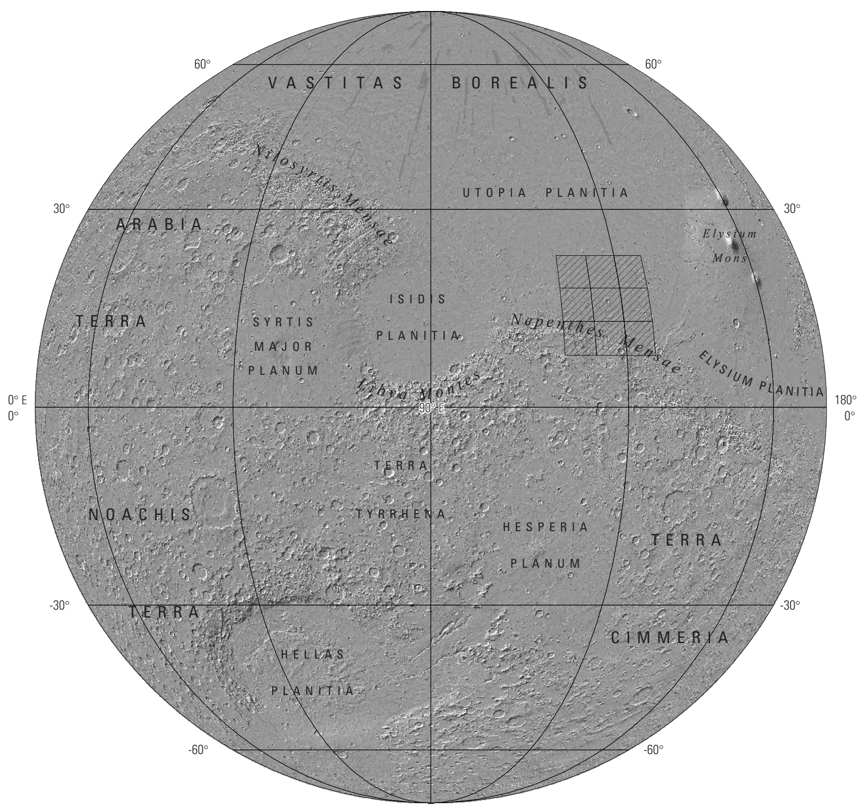

Map showing the location of the Nepenthes Planum region (Mars Transverse Mercator (MTM) 10237, 10242, 10247, 15237, 15242, 15247, 20237, 20242, and 20247 quadrangles; hachured region) and major physiographic features. Image is Mars Orbiter Laser Altimeter (MOLA) artificial hillshade overlain on a Thermal Emission Imaging System (THEMIS) daytime infrared (IR) mosaic. Orthographic projection centered at long 90° E.

2018

U.S. Department of the Interior
U.S. Geological Survey

Contents

Table

Introduction

One of the most dominant topographic features on the surface of Mars is the highland-lowland transition, a globe-encircling feature, which separates geologically ancient, higher-standing and densely cratered plateaus from the relatively younger, lower-lying and sparsely cratered plains by 1–5 kilometers (km). The morphologic expression of this feature is laterally variable, ranging from a very shallow (<0.1°), north-sloping, cratered surface in northern Arabia Terra (lat 30.0 to 46.0° N, long –8.0 to 20.0° E) to a topographic scarp bounded by eroded remnants of highland plateaus and knobs in Nilosyrtis Mensae (lat 28.0 to 45.0° N, long 32.0 to 80.0° E). Intermediate within this morphologic continuum is the highland-lowland transitional zone, which separates the cratered highlands of Terra Cimmeria in the south from the low-lying plains of Utopia Planitia in the north. This region has been interpreted to be underlain by deeply seated crustal faults associated with the formation of the giant Utopia multi-ring impact basin (McGill, 1989; Frey and Schultz, 1990; Tanaka and others, 2003a, 2005; Nimmo and Tanaka, 2005), which may have controlled not only the regional accumulation of rocks and sediments but also the trapping and transport of subsurface water and (or) ice reservoirs over a long period of Mars' geologic history (Tanaka and others, 2003b; Skinner and Tanaka, 2007). A more complete understanding of the range of geologic processes that have operated within the highland-lowland transitional zone is now possible because of modern (post-Viking Orbiter) data sets, in particular higher-resolution images, which support more detailed geologic observations that are presented in this map. In turn, material units and modificational features can be dated with more precision based on stratigraphic relations and crater-density data. The map results permit new interpretations of the origin and age of geologic materials and features and a reconstruction of the geologic history that provides an improved understanding of the development of the highland-lowland transition zone and northern plains in the Nepenthes Planum region. The map also provides geologic and stratigraphic context for future studies within the Nepenthes Planum region, as well as comparative areas along the highland-lowland transitional zone.

The highland-lowland transitional zone located between Terra Cimmeria and Utopia Planitia was first mapped as part of the Amenthes quadrangle by Hiller (1979) using Mariner 9 images at 1:5,000,000 scale. Hiller (1979) identified two main physiographic and geologic subdivisions in the region: the higher-standing, densely cratered plateau located to the south and sparsely to moderately cratered plains located to the north. Therein, he subdivided the densely cratered plateaus into "hilly and cratered material" and "cratered plateau material," representing ancient Martian crustal materials or lava plains burying such materials. Moderately cratered plains were similarly subdivided into "cratered plains materials" and "smooth plains materials" (Hiller, 1979). The occurrence of discontinuous lobate scarps within the "smooth plains" unit prompted Hiller (1979) to interpret that unit as volcanic plains consisting of low-viscosity lava flows, geologically and morphologically comparable to lunar maria. The prominence of impact craters with diverse geomorphological expression was interpreted as evidence of various levels of erosional modification and, thus, increasingly older unit age from north to south (Hiller, 1979).

A composite of the 1:5,000,000-scale quadrangles—including an early version of the Amenthes quadrangle geologic map of Hiller (1979)—resulted in a 1:25,000,000-scale global geologic map of Mars based on Mariner 9 images (Scott and Carr, 1978). This map was the first to assign chronostratigraphic ages to geologic units on Mars. Therein, Scott and Carr (1978) grouped the smooth, generally lower standing cratered plains material into the Amazonian System, the knobby terrains that morphologically define the northern margin of the cratered highlands into the Noachian and Hesperian Systems, and the rugged, generally higher standing cratered plains to the Noachian System.

Applying the stratigraphic framework of Tanaka (1986), Greeley and Guest (1987) used the improved areal coverage and spatial resolution of Viking Orbiter images to produce a 1:15,000,000-scale geologic and geomorphologic map of the eastern equatorial region of Mars that includes the Terra Cimmeria-Utopia Planitia highland-lowland transitional zone. These mapping geologists refined the occurrence of the "smooth plains" unit of Scott and Carr (1978) by differentiating an east-west-oriented outcrop of Amazonian "knobby plains material," which they interpreted as sedimentary or volcanic plains surrounding eroded vestiges of crustal massifs and (or) localized volcanic vents. Greeley and Guest (1987) mapped Hesperian "ridged plains material" directly south of the knobby plains, interpreting that unit as low-viscosity lava plains deformed by thrust faults related to global contraction. Though only partly documented by the Mariner 9-based geologic maps, Greeley and Guest (1987) discriminated an east-west swath of isolated and coalesced shallow depressions within the ridged plains material in the Terra Cimmeria-Utopia Planitia transitional zone. They described these as Amazonian to Hesperian "etched plains material" and interpreted them as accumulations of aeolian sediments that were subsequently scoured by wind. South of the ridged and etched plains materials, Greeley and Guest (1987) mapped the rugged plateaus, mesas, and knobs that make up the areal bulk of the regional highland-lowland transition scarp as the Hesperian and Noachian "undivided material", interpreted as irresolvable collections of eroded highland rocks. Greeley and Guest (1987) identified the cratered highlands of northern Terra Cimmeria as the Noachian "dissected unit" of the plateau sequence. The bulk of the units in the cratered highland were interpreted as laterally varying proportions of impact breccias and intercalated volcanic and (or) sedimentary rocks, some of which were subsequently dissected by fluvial processes.

Tanaka and others (2005) used topographic and image data sets from instruments onboard the Mars Global Surveyor (MGS) and Mars Odyssey (ODY) orbiting spacecraft to refine the geologic and stratigraphic context of the Martian northern plains at 1:15,000,000 scale. Therein, units were differentiated, where possible, based on depositional and (or) erosional hiatuses (unconformities). This approach resulted in the identification of two discrete units associated with the cratered highlands (the Libya Montes and Noachis Terra units), three units associated with the highland-lowland transitional zone (the Nepenthes Mensae and Utopia Planitia 1 and 2 units), and two units associated with the broader lowland plains (the Vastitas Borealis marginal and interior units) (Tanaka and others, 2005). Southern Utopia Planitia was used as the type locality for highland-lowland boundary units (Tanaka and others, 2005).

The northern plains map served as a precursor to a new global geologic map of Mars at 1:20,000,000 scale, which also used an increased volume of data obtained by MGS and ODY as well as image and other data from the Mars Express (MEX) and Mars Reconnaissance Orbiter (MRO) spacecraft (Tanaka and others, 2014). However, because of a revised unit grouping and naming scheme and the reduced scale, the global map employs different units. Globally occurring units that are depicted by Tanaka and others (2014) are geologically and stratigraphically comparable to hemispherically occurring units of Tanaka and others (2005). These include Middle Noachian massif unit (comparable to (~) the Libya Montes unit of Tanaka and others (2005)), Early Noachian and Middle Noachian highland units (~Noachis Terra unit), Hesperian and Noachian transition unit (~Nepenthes Mensae unit), Early and Late Hesperian transition units (~Utopia 1 and 2 units), and Late Hesperian lowland unit (~Vastitas Borealis marginal and interior units). Both maps include the north-trending wrinkle ridges and scarps named Hephaestus Rupēs, which occur in Amazonian and Hesperian geologic units.

The Nepenthes Planum region has been targeted as a favorable landing site for several landed missions to Mars because of its low-latitude position, pervasive planarity, and relatively low elevation. The backup landing site for Viking Lander 1 was the (informally named) Tritonis Lacus albedo region within Nepenthes Planum (lat 20.0° N, long 108.0° E) (Masursky and Crabill, 1981). Nepenthes Planum was again discussed as a final candidate landing site for the 1997 Mars Pathfinder mission (lat 20.0° N, long 108.0° E; Golombek and others, 1997), the 2001 European Space Agency's Beagle 2 mission (lat 20.0° N, long 114.0° E; Bridges and others, 1999), and the 2004 Mars Exploration Rover mission (lat 11.7° N, long 124.0° E; Tanaka and others, 2003b). Though the region met all data and mission safety requirements, the overarching perception in each of these instances was that the geologic character of the Nepenthes Planum region remained poorly understood (relative to other candidate landing sites), making potential science discovery difficult to assess.

Despite nonselection, the targeted examination of subregions within the Nepenthes Planum region resulted in an inordinate volume of specialized observations and topical science investigative results, which are useful for unraveling the regional geologic story. These results are particularly relevant to deciphering not only the largely planar units that make up the southern Utopia Planitia and, by extension, the broader northern plains of Mars, but also the undulating terrains that makeup the highland-lowland transition in the Nepenthes Planum geologic map region. Regarding the planar units within southern Utopia, Clifford and Parker (2001) notably used original landform mapping by Parker and others (1993) to postulate that the Martian northern plains are broadly encircled by two laterally continuous topographic benches, high albedo lobes, and arcuate ridges. These researchers interpreted these features as vestiges of shorelines formed by highstands of a northern ocean filled by water and sediment sourced through the circum-Chryse Planitia outflow channel (Parker and others, 1993; Clifford and Parker, 2001). The lower of these two features, termed the "Deuteronilus shoreline" (Clifford and Parker, 2001), coincides with the southernmost margins of the Vastitas Borealis Formation of Greeley and Guest (1987) and the Vastitas Borealis marginal unit of Tanaka and others (2005). This putative shoreline transects the northernmost part of the Nepenthes Planum map area. Despite multiple mapping and topical science investigations conducted subsequent to the original, pioneering work by Parker and others (1993; for example, Head and others, 1998; Kreslavsky and Head, 2000; Kreslavsky and Head, 2002; Carr and Head, 2003; Tanaka and others 2005; Ghatan and Zimbelman, 2006; Ivanov and others, 2014), the existence, origin, and fate of a putative ocean in the Martian northern plains, the margins of which transect the Nepenthes Planum map region, remain mostly unresolved.

Regarding the origin of Nepenthes Planum, which represents the regional physiographic and topographic transition from the cratered highlands of Terra Cimmeria to the lowland plains of Utopia Planitia, Skinner and Tanaka (2007) mapped, along the southern margin of Utopia Planitia, Hesperian fractured rises, elliptical mounds, pitted cones, and cavi depressions proposed to be a suite of features potentially formed through the ascent of sedimentary diapirs and associated subsidence of adjacent planar sedimentary plains, similar to terrestrial mud volcanic processes (for example, Kopf, 2002). These researchers interpreted that these features collectively attested to possible accumulations of water-saturated sediments within structural rings of the Utopia basin. Brož and Hauber (2013) presented an alternative interpretation to the mud volcano-like hypotheses of Skinner and Tanaka (2007). These researchers studied the morphologic and morphometric shapes of pitted cones in and around Nepenthes Planum (and other regions) and speculated that these features are very similar to terrestrial hydrovolcanic tuff rings and cones, implying a juvenile magamatic origin. The two contrary perspectives offered by Skinner and Tanaka (2007) and Brož and Hauber (2013) illustrate the ambiguity inherent to remote-based interpretations of Martian landforms and underscore a need for objective context afforded by scale-based geologic mapping.

As summarized above, the systematic observation, mapping, and topical investigation of the geology in the highland-lowland transitional province on Mars result in complex, varied, and often contradictory interpretations of the evolutionary history for this region. The local to regional evolution of the rocks and sediments of the Nepenthes Planum region, particularly those of intermediate (Hesperian) to young (Amazonian) age, remain poorly understood. Herein, we discriminate and describe the geologic and stratigraphic units of Nepenthes Planum as well as the bounding cratered southern highlands and low-lying northern plains and provide an evolutionary history based on geologic mapping, which can be compared and contrasted with other sections of the Martian highland-lowland transitional province.

Geography

Our mapping efforts focused on the geomorphic terrains and geologic units contained within Mars Transverse Mercator (MTM) 10237, 10242, 10247, 15237, 15242, 15247, 20237, 20242, and 20247 quadrangles. These quadrangles are located in the eastern hemisphere of Mars and span 15° of latitude (lat 7.5 to 22.5° N) and 15° degrees of longitude (long 110.0 to 125.0° E). The map region, defined by the above quadrangles, is centered on Nepenthes Planum (fig. 1), a smooth to rolling, slightly north-sloping plain that forms the physiographic transition from higher-standing cratered highlands of northern Terra Cimmeria to the south and the lower-standing, relatively sparsely cratered lowlands of southern Utopia Planitia to the north. Nepenthes Mensae are located to the south of Nepenthes Planum and are defined by east-west-oriented collections of closely spaced plateaus, mesas, and knobs as well as their intervening plains. The Amenthes Cavi are located to the north of Nepenthes Planum and are defined by east-west-oriented arrays of isolated and coalesced depressions with arcuate, rounded to scarp-like margins. Amenthes Cavi demarcate the southern margin of Utopia Planitia, a >3,000-km-diameter, plate-shaped depression centered north of the map area near lat 46.4° N, long 113.1° E. North-south-oriented scarps and ridges of the Hephaestus Rupēs occur in the central and northern part of the map region. Northwest-southeast-oriented fractures of Hephaestus Fossae cross the map region in the northeast. The Nepenthes Planum region contains multiple large-diameter impact craters, including Ehden (57.4 km diameter), Canillo (33.9 km), Tavua (31.6 km), Zaranj (27.4 km), Doba (25.9 km), Marbach (24.7 km), Phedra (20.3 km), and Linpu (18.2 km). As a candidate for the Viking missions landing site, focus on the region resulted in the naming of several small-diameter impact craters in the northwest part of the map region. Additionally, several dark-rayed craters—suggestive of relatively young, rocky ejecta—are named in the eastern part of the map region.

Base Map and Data

The extensive spatial coverage, high resolution, and diversity of post-Viking Orbiter data sets allow more detailed discrimination and analysis of the geologic materials and landforms that occur within and around Nepenthes Planum. Moreover, these data sets offer an improved context for interpreting the formational history of this and other highland-lowland transitional zones. Though photogeology and geomorphology continue to define the cornerstone of planetary geologic mapping (for example, Greeley and Batson, 1990), new techniques are required to most appropriately convey stratigraphic and structural relations, particularly at scales that adapt and merge multiple MTM quadrangles. Below, we describe the (1) characteristics of the primary geologic base map and (2) relevance and use of supplemental (secondary) data sets.

The primary base map used for this geologic map is composed of daytime thermal infrared (IR) images acquired by the ODY-borne Thermal Emission Imaging System (THEMIS) camera (Christensen and others, 2004) and compiled into a 100-meter-per-pixel (m/px) mosaic by the U.S. Geological Survey Astrogeology Science Center. We augmented the THEMIS daytime IR base map with a 128 pixels/degree (~463 meters/pixel) digital elevation model (DEM) interpolated from 300-m footprint surface altimetry measurements acquired by the MGS-borne Mars Orbiter Laser Altimeter (MOLA) instrument (Smith and others, 2001). The geologic units that are mapped and described herein are geodetically tied to the THEMIS base map and MOLA DEM due to their full areal coverage of the selected quadrangles. We used Transverse Mercator projection with a center longitude of 110° E for all base data.

Though primary map bases establish the most critical contextual information needed to correlate geologic units and consistently map their bounding contacts and characteristics, we corroborated mapping results by integrating other data sets, including MOLA-derived products (in particular shaded-relief maps with color elevation scales) as well as the full range of ODY THEMIS visual, MGS Mars Orbiter Camera (MOC), MRO High Resolution Imaging Science Experiment (HiRISE), and MRO Context Camera (CTX) images via web-linked image footprints in a geographic information system (GIS) project. Though these data sets provided important information regarding unit texture and stratigraphic relations, they were considered supplemental because they provided neither complete areal coverage nor resolution compatible for discriminating discrete units at the publication map scale. Supplemental data sets were used to augment the accompanying Description of Map Units where clear and consistent textural and (or) stratigraphic characteristics were observed (table 1).

Methodology

We constructed the geologic map of the Nepenthes Planum region using methods that both follow and deviate from the approaches described by Tanaka and others (2005) for the hemisphere-scale geologic map of the northern plains of Mars. Below, we describe (1) unit groups, names, and symbols, (2) types of geologic contacts, (3) types of feature symbols, and (4) digital drafting parameters used to compile information.

Unit Groups, Names, and Labels

We name the geologic units that occur within the Nepenthes Planum region using terms that are either based on a pervasive landform or a particular genesis, where possible, in order to preserve objectivity (Salvatore, 1994; Hansen, 2000; Tanaka and others, 2005). Tanaka and others (2005) subdivided the Martian northern plains into specific geographic divisions and uniquely named and labeled the geologic units that occurred within these provinces as a means to partition the regional geologic histories and simplify description. In that map, the Nepenthes Planum region extends from highland terrains defined as “widespread materials” by Tanaka and others (2005) into the “Borealis province” of the northern plains. In contrast,

Table 1. Characteristics of geologic units in the mapped Nepenthes Planum region, Mars: areas, crater densities, and superposition relations.

[N(1), number of craters ≥1km in diameter per million square kilometers; N(5), number of craters ≥5km in diameter per million square kilometers; N(16), number of craters ≥16km in diameter per million square kilometers; —, not applicable or no data]

Unit Name	Unit label	Unit Area (Count Area)[1] 103 km^2	N(1)	N(5)	N(16)	Crater-density age[2]	Superposition relations[3]
			Lowland Province/Utopia Region Units				
Utopia 2 unit	AHlu$_2$	152.3 (154.8)	1,524.7±99.3	64.6±20.4	—	lH–eA	<Hlu$_1$, Htn$_f$, AHc; >AHc
Utopia 1 unit	Hlu$_1$	155.9 (168.0)	1,423.0±92.0	83.4±22.3	23.8 ±11.9	lH–eA	<Htn$_v$, Htn$_f$, Nhc$_1$, AHc, AHce$_a$, AHce$_b$; >AHlu$_2$, AHc, AHce$_b$
			Transitional Province/Nepenthes Region Units				
Nepenthes vent unit	Htn$_v$	2.5 (2.5)	3221.6±1,139.0	—	—	—	~Htn$_f$; >Hlu$_1$, AHc
Nepenthes flow unit	Htn$_f$	228.3 (292.8)	2,994.9±101.1	170.7±24.1	17.1±7.6	eH	<HNhc$_3$, Nhc$_1$, AHc; ~Htn$_v$; >Hlu$_1$, AHc, AHce$_a$, AHce$_b$
			Highland Province/Cimmeria Region Units				
Cimmeria 3 unit	HNhc$_3$	24.0 (31.2)	2,983.8±309.4	224.6±84.9	96.3±55.6	lN–eH	<Nhc$_2$, Nhc$_1$; >AHc, AHce$_a$, AHce$_b$
Cimmeria 2 unit	Nhc$_2$	20.8 (21.6)	3,048.9±375.3	231.0±103.3	92.4±65.3	lN–eH	<Nhc1; >Nhc2,, AHc, AHceb
Cimmeria 1 unit	Nhc$_1$	42.1 (68.9)	2,958.7±207.1	290.1±64.9	43.5±25.1	lN	>Hlu$_1$, Htn$_f$, HNhc$_3$, Nhc$_2$, AHc, AHce$_a$, AHce$_b$
			Widely Occurring/Impact Crater Units				
Crater material, undivided	AHc	38.6	—	—	—	—	<AHlu$_2$, AHc, Hlu$_1$, Htnv, Htnf, HNhc$_3$, Nhc$_2$, Nhc$_1$, AHce$_a$, AHce$_b$, AHcw, AHcf, AHcp; >AHlu$_2$, Hlu$_1$, AHc, Htn$_f$, AHce$_a$ AHce$_b$
Crater ejecta, facies a (inner)	AHce$_a$	36.0	—	—	—	—	~AHce$_b$, AHcr; >Hlu$_1$, Htn$_f$, Nhc$_3$
Crater ejecta, facies b (outer)	AHce$_b$	49.5	—	—	—	—	< Hlu$_1$, Htn$_f$, HNhc$_3$, Nhc$_2$, Nhc$_1$, AHce$_a$, AHce$_b$; ~ AHce$_a$, AHcr, AHcw, AHcf AHcp; >Hlu$_1$, Htn$_f$, AHce$_b$, AHc
Crater rim	AHcr	5.1	—	—	—	—	~AHce$_a$, AHcw, AHcf; >AHc
Crater wall	AHcw	3.3	—	—	—	—	~AHcr, AHcf, AHcp; >AHc
Crater floor	AHcf	2.1	—	—	—	—	~AHcw, AHcp, AHcr; >AHc
Crater peak	AHcp	0.5	—	—	—	—	~AHcw, AHcf; >AHc

[1] Count Area represents the unit area combined with the overlying impact crater units. See Age Determinations for details.

[2] Based on crater-density boundaries as determined by Werner and Tanaka (2011). A, Amazonian; H, Hesperian; N, Noachian; e, Early; m, Middle; l, Late.

we denote our map regions as parts of global-scale geographic provinces (highland, transitional, lowland, and widely occurring) as indicated in the Correlation of Map Units. To assist with geographic, geologic, and stratigraphic description, we group geologic units of this map into three discrete geographic regions based on nomenclature approved by the International Astronomical Union (IAU): the Cimmeria, Nepenthes, and Utopia region units. The Cimmeria region units are those that comprise the rugged, high-standing massifs and large-diameter impact craters and basins that extend from approximately –300 m elevation in the southern part of the map region to approximately –1,300 m elevation along the northern margin of Nepenthes Mensae (fig. 1). The Nepenthes region units are those that comprise the undulating, locally smooth to rugged plains that extend from approximately –1,300 m elevation along the northern margin of Nepenthes Mensae to approximately –3,300 m along the northern margin of Amenthes Cavi. The Utopia region units are those that comprise the nearly horizontal, low-lying plains that extend from approximately –3,300 m along the northern margin of Amenthes Cavi to approximately –3,900 m in the northern part of the map region.

The approach summarized above refines organizational efforts by Tanaka and others (2005) in two fundamental ways. First, we intentionally partition the geologic units that define the highland-lowland transitional zone, which allows for their description as geologically and stratigraphically unique entities. Second, we assign each geographic region names that correspond to their nearest (and largest) regional feature, which allows for comparison of geographically, and perhaps geologically, discrete regions along the globe-encircling highland-lowland transitional scarp. These groupings are shown in the COMU.

We name the units of the Nepenthes Planum map region based on their geographic occurrence as well as their stratigraphic relations to one another. We identify fourteen geologic units in the map region, as follows: two units of the Utopia region of the lowland province, two units of the Nepenthes region of the highland-lowland transitional province, three units of the Cimmeria region of the highland province, and seven impact crater units. The Utopia region units consist of the Utopia lowland 1 and 2 units. The Nepenthes region units consist of the Nepenthes transitional vent and flow units. The Cimmeria region units consist of the Nepenthes highland 1, 2, and 3 units. Impact crater units consist of the crater undivided, ejecta facies a (inner), ejecta facies b (outer), rim, wall, floor, and peak units.

We assign each mapped unit a label that uniquely identifies the chronologic period(s) in capital form (H, Hesperian Period). Next, for non-crater units, the geographic province in lower-case form (l, lowland province), followed by the geographic region in lower-case form (u, Utopia region). Crater units are indicated by a lower-case c. An additional descriptor is used as a subscript when it is necessary to identify either the interpreted stratigraphic order for closely related units (1, oldest of two or more sequentially emplaced units) or primary emplacement morphology (v, eruptive vent unit). Units that have morphologic descriptors are interpreted to have been emplaced contemporaneously. As examples, under this scheme, the geologic label "Nhc_1" refers to the Noachian-age, stratigraphically lowest unit that occurs in the Cimmeria region of the Martian highlands, and the geologic label "Htn_v" refers to the Hesperian-age eruptive vent unit that occurs in the Nepenthes region of the Martian highland-lowland transition. Finally, materials of craters >16 km in rim diameter are divided into structural components (rim, wall, floor, peak, and ejecta) that require an additional small letter symbol, and the ejecta are subdivided into two morphologic facies—facies a (inner) and facies b (outer)—indicated as subscripts.

Contact Types

We delineate geologic units within the map region using contacts that are attributed with their interpreted level of certainty in identification and spatial placement as well as their geologic occurrence. A certain contact denotes the most precise contact between well-characterized geologic units that contrast in appearance and (or) interpreted relative age. In some instances, certain contacts have hachures to denote unit margins that are defined by lobate scarps (hachures on downslope side of contact). These are always assigned to certain contacts. An approximate geologic contact is regarded as less precise in its identification and (or) spatial placement due to data quality, subtlety of contact, and (or) obscuration by secondary processes.

Feature Types

The map includes a variety of morphologic feature symbols, following precedents established in previous terrestrial and planetary geologic maps. We subdivide our mapping of some features as indicated in the Explanation of Map Symbols. Although consistent mapping of features is desired, it is generally not possible or practical due to complications that can arise from (1) locally rugged terrain; (2) variation in feature character, length, and (or) relief; (3) feature orientation relative to illumination (for smaller features not resolved in MOLA data); and (4) areas of low data resolution and (or) incomplete data coverage. The features we mapped commonly grade in appearance and overlap in places and should be considered cartographic representations rather than exact in regard to spatial location and abundance. Linear features include ridges, troughs, scarps, and crater rims. Point features include pitted cones (discriminated by size) and mounds. A single polygon feature was mapped on unit Htn_f to indicate rugged surface textures, which grade across this unit in the map region.

Digital Drafting Parameters

We used the Esri (v. 10.1, 1982–2013, Redlands, CA) ArcGIS to co-register and analyze available datasets. We digitized points, lines, and polygons using the digital streaming capability in ArcGIS. We digitized vector linework at a consistent scale of 1:250,000 (600 percent of the publication map scale), which allowed for substantially detailed lines for use in both hard-copy map publication, as well as a digital product, while remaining true to the publication map scale of 1:1,500,000. Vertex spacing was set to place points within linework at 250 m (1 vertex per 1 millimeter (mm) at 1:250,000 digitizing map scale).

Linework was streamed using a WACOM Intuos 3 digital mapping tablet into an ArcGIS digital geodatabase in Transverse Mercator projection (center longitude of 110° E). The geodatabase housed the attribute information for each digitized feature, which was assigned iteratively using attribute domain settings stored within the geodatabase. Geologic map symbols are based on Federal Geographic Data Committee Digital Cartographic Standards for Geologic Map Symbolization (Federal Geographic Data Committee, 2006). Iterations of the digitized linework allowed for refinement of contact placement and unit descriptions based on cross-comparison between the map base and supplemental data sets. Contact linework was cleaned (dangles removed) and used to build unit polygons. To balance base map resolution and clear, consistent cartographic representation, all unit outcrops are >7 square kilometers (km^2) and line features are >3 km long, effectively representing a 2 mm lower limit at map scale for polygon and line features. Points features are based on the resolution of the THEMIS and MOLA base maps and are considered to be >500 m in diameter.

Geomorphology

The spatial and morphologic characteristics of landforms that occur within the geologic units of the Nepenthes Planum region provide information that aids in discerning the regional geologic history.

Ridges

We identify two types of ridges in the map region. A crenulated (wrinkle) ridge is a sub-linear landform whose crest is defined by singular or en echelon sets of prominent to subdued crenulations (that is, “wrinkles”). Crenulated ridges are commonly asymmetric in topographic profile and have dominant east-west and north-south orientations, though directional trends vary across the map region. North-south oriented crenulated ridges are most prominent within and north of Nepenthes Planum, where they define the axes of elongated topographic arches and parallel north-south outcrops of the Nepenthes flow unit (Htn_f). These make up the southern extents of the Hephaestus Rupēs (fig. 1). Crenulated ridges generally rise 50 to 100 m above surrounding plains, though taller features occur locally. These features are generally between 3 and 5 km wide, with the widest portion occurring near the middle of the observable length. These types of ridges form a notable reticulate pattern in the Cimmeria 3 unit ($HNhc_3$) located east of long 120° E. We mapped 434 wrinkle ridges within the map region ranging in length from 3.1 to 52.1 km (13.1 km mean).

A narrow, arcuate ridge is a <500-m wide, sub-linear to curving landform that most commonly occurs in nested sets with ridges of similar shape and orientation. These features appear to be <10 m tall, though the accuracy of these values are difficult to ascertain because feature width is comparable to the spatial resolution of topographic data. Narrow, arcuate ridges are composed of and (or) occur in close proximity to small diameter pitted cones (described below). Narrow, arcuate ridges occur exclusively in the Utopia 2 unit ($AHlu_2$), typically within 100 km of its contact with the Utopia 1 unit (Hlu_1). Therein, features commonly link low-relief knobs and plateaus of the Nepenthes flow unit (Htn_f; fig. 2). We mapped 828 narrow, arcuate ridges within the map region ranging in length from 3.0 to 16.2 km (4.9 km mean).

Depressions

We identify three types of negative relief landforms in the map region. A subdued groove is a linear to sub-linear, shallow-walled depression. These features occur in the Nepenthes flow unit (Htn_f) in Nepenthes Planum as well as around the central depressions of Amenthes Cavi. Troughs also occur in plateaus and mesas of the Cimmeria 1 unit (Nhc_1) in northern Terra Cimmeria and Nepenthes Mensae. Troughs are generally <1 km wide (though locally wider features are common in highland units) and <10 m deep, though these features may locally be several tens of meters deep. We mapped 325 troughs in the map region ranging in length from 3.0 to 40.0 km (6.1 km mean).

A trough is a linear to sub-linear, steep-walled depression that ranges from several tens of meters to up to several hundreds of meters in depth. These features occur in the northeast part of the map region and collectively form the Hephaestus Fossae. Troughs trend northwest-southeast and northeast-southwest and are oriented orthogonal to one another, forming a characteristic polygonal pattern. These features are located entirely in the Utopia 1 and 2 units ($AHlu_2$ and Hlu_1, respectively). Grooves are both continuous and discontinuous, the latter occurring as linear segments connected by narrow septa (fig. 3). These types of troughs occur between –3506 and –3908 m elevation, with discontinuous segments becoming more frequent to the northwest and at lower elevation. We mapped 322 grooves in the map region ranging in length from 3.0 to 134.4 km (11.0 km mean).

A channel is mapped herein as the axis of a valley that has a sinuous to anastomosing planimetric shape and that tends to merge with like features in the downslope direction. Channels occur in shallow highland basins in the Cimmera 2 and 3 units (Nhc_2 and $HNhc_3$, respectively) along the highland margin of the highland-lowland transitional zone (fig. 4). Channels can locally be positioned on positive relief segments (fig. 5). We mapped 42 channel troughs in the map region ranging in length from 3.5 to 23.3 km (8.1 km mean).

Scarps

We identify two types of topographic scarps in the Nepenthes Planum region. A base of scarp identifies the basal topographic inflection of a linear to curving, sharp to subdued scarp. In northern Terra Cimmeria, scarp bases occur individually and as sets that define the margins of east-west trending massifs (roughly parallel to the highland-lowland boundary scarp). Scarp bases between Amenthes Cavi and southern Utopia Planitia occur parallel and in close spatial association with north-south trending crenulated ridges and outcrops of the Nepenthes flow unit (Htn_f). In the plains of southern Utopia Planitia, scarp bases occur in arcuate segments that outline shallow, circular depressions. We mapped 155 scarp bases in the map region ranging in length from 4.0 to 38.5 km (11.9 km mean).

A lobate scarp is a topographically subtle, curving scarp that defines the margins and terminations of lobes that are generally <10 m tall. These features occur predominantly in the Nepenthes flow (Htn_f) as well as in the Utopia 2 unit ($AHlu_2$) near the contact with the Utopia 1 unit (Hlu_1). Lobate scarps also locally define geologic contacts throughout the map region. We mapped 198 lobate scarps in the map region ranging in length from 4.5 to 67.8 km (14.3 km mean).

Pitted Cones and Mounds

We identify two types of positive relief landforms within the map region. A pitted construct is a conical landform that contains a central pit or depression. We subdivide the regional population of pitted constructs based on the basal diameter of observed features. A small pitted construct is generally between 500 m and 1.0 km in diameter, has sloping flanks, and appears to have a central pit that is near the limit of the THEMIS base map resolution (fig. 2). Small pitted constructs are either isolated or aligned and occur almost entirely in the Utopia 2 unit ($AHlu_2$), often in close association with narrow, arcuate ridges (see Scarps). A few of these features are mapped within the Utopia 1 unit (Hlu_1) within the Amenthes Cavi. We mapped >3300 of the small pitted constructs in the map region.

Large pitted constructs are from 1.9 to 9.1 km in diameter (4.8 km mean), have sloping or rounded flanks, and have a central pit with a diameter that is commonly >50 percent of the feature's total basal diameter (fig. 6). Large pitted constructs are either isolated or coalesced and either circular or crescentic in planimetric shape. They occur almost entirely in the Nepenthes flow unit (Htn_f) west of long 119° E. Several features occur in the depressions of Amenthes Cavi where they are surrounded by the smooth plains of the Utopia 1 unit (Hlu_1). We mapped 75 large pitted constructs in the map region.

Small tholi (that is, mounds) range from 2.0 to 6.6 km in diameter (4.7 km mean) and have marginal scarps, subtle interior slopes, circular to ovoid planimetric shape, and in some cases central peaks (fig. 7). Mounds are most often isolated rather than coalesced and occur entirely in the Nepenthes flow unit (Htn_f), south of the Amenthes Cavi, often adjacent to wrinkle ridges. We mapped 109 mounds in the map region.

Surface Texture

We identify a single texture—rugged surface—within the map region, which is confined entirely to the transitional Nepenthes flow unit (Htn_f). These surfaces are pitted and hummocky at THEMIS base map resolution (fig. 6), grade laterally into smoother surfaces within unit Htn_f, and occur entirely west of long 118° E in Nepenthes Planum. We mapped 22 discrete occurrences of the rugged surface in unit Htn_f, with areas ranging from approximately 20 to >38,000 km^2 (45,716 km^2 total).

Age Determinations

The cumulative densities of impact craters greater than specified diameters provide some stratigraphic control and temporal constraint (table 1), as do crosscutting and superposition relations. Crater densities were derived for non-crater units using computed map areas and a project-specific catalog of all craters ≥1 km in diameter. (Crater units were not counted since each crater represents an isolated event, and the occurrences are generally too small in areal extent for reliable statistical results.) Craters within this size range were catalogued using a three-point tool to measure impact crater rim diameters. Crater rims were identified on the THEMIS base map and verified/refined where necessary using MOLA topography and derived products. Map units were assigned to the eight Martian epochs on the basis of the scheme of Tanaka (1986) as updated by Werner and Tanaka (2011) for the number of craters ≥1, 5, and 16 km in diameter per million square kilometers (N(1), N(5), and N(16), respectively), as well as on stratigraphic relations. Unit areas, crater densities, crater-density ages, and superposition relations with contiguous units are presented in table 1.

Our unit age assignments take into account first and foremost unit superposition relations observed and interpreted from mapping observations, which define the sequence of unit emplacement. Crater-density ages, primarily from our results (table 1), but also in consideration of regional crater counts having less statistical error but more geologic uncertainty (Tanaka and others, 2005, 2014; Werner and Tanaka, 2011), provide some calibration to the age assignments. The crater-density ages provide a mean surface age, even though some units may have been emplaced over a considerable time span. In addition, smaller craters can be destroyed by later modification, yielding younger surface ages for smaller craters (see Platz and others, 2013). For the Nepenthes Planum region, the N(1) crater densities consistently yield younger ages than N(5) ages and thus do not appear to be reliable for assigning unit emplacement ages.

The Cimmeria 1 unit has a Late Noachian crater density that is even lower than that of the Cimmeria 2 unit, but in the map region it is composed of remnants that we interpret were being emplaced and modified during the Hesperian. As such, we suggest that the age for the Cimmeria 1 unit is better reflected in ages determined from regional and global mapping (Tanaka and others, 2014), which are Early to Middle Noachian. The Cimmeria 2 unit is assigned to the Middle to Late Noachian, which is consistent with N(5) and N(16) crater densities and superposition relations. The Cimmeria 3 unit overlies the Cimmeria 2 unit and its larger crater densities are consistent with a Late Noachian to Early Hesperian age. The Nepenthes flow unit has an N(5) age and stratigraphic relations consistent with an Early Hesperian age. The Nepenthes vent unit is coeval with the Nepenthes flow unit. The Utopia 1 unit has a Late Hesperian age based on both crater density and superposition relations with regional to global units (Tanaka and others, 2014). The Utopia 2 unit has a mean N(5) age at the Hesperian/Amazonian boundary. The mapped crater units all represent cases of craters with well-preserved rims and ejecta, which indicate that they post-date globally high rates of erosion that terminated at the end of the Noachian Period. In some cases, particular craters have superposition relations with map units that provide some age constraint. Units derived from Ehden crater appear to be embayed by the Cimmeria 3 unit and are thus likely to have been emplaced during the Early Hesperian. Units derived from Marbach, Phedra, and Tavua craters superpose the Nepenthes flow unit and are embayed by the Utopia 1 unit, indicating that they were likely emplaced during the Early to Late Hesperian. Units derived from Linpu crater show no clear indication of embayment by the Utopia 1 unit, implying emplacement during the Late Hesperian or Early Amazonian (or perhaps later).

Geologic Summary

In this section we summarize the geologic history of the Nepenthes Planum highland-lowland transitional province of Mars based on the geologic unit and landform mapping and stratigraphic determinations presented herein. This summary is portrayed graphically in the accompanying Correlation of Map Units.

Noachian Period

The recorded geologic history of the Nepenthes Planum region of Mars begins in the Early to Middle Noachian during which the Cimmeria 1 unit (Nhc_1) was emplaced. The Cimmeria 1 unit likely represents regolith composed of impact breccia and melt, volcanic rocks, and clastic sedimentary rocks of aeolian, alluvial, mass wasting, and other geologic materials of undetermined origins. Crater densities indicate the unit Nhc_1 post-dates the formation of the Utopia multi-ring impact basin, which impacted into rocks that likely underlie the oldest exposed Noachian rocks within the map region. The Cimmeria 1 unit outcrops are oriented sub-parallel to the regional east-west orientation of the highland-lowland transitional scarp, raising the possibility that some of these outcrops are impact-modified massifs uplifted by the crater- and basin-forming impact events, specifically the Utopia impact. Lithologic and (or) depositional characteristics that may indicate the direct origin of the rocks and sediments within the unit Nhc_1 are altogether absent. They are generally interpreted to represent degraded crustal rocks and highland regolith that were perhaps subsequently modified by mass-wasting processes along the highland-lowland transitional scarp. Unit Nhc_1 is separated from the Cimmeria 2 unit (Nhc_2) based on topographic inflections, wherein the older unit is generally characterized by high -relief, rugged outcrops. The stratigraphic nature of the contact between units Nhc_1 and Nhc_2 is likely of embayment given its general topographic form, though high-resolution images demonstrate that clear evidence of embayment is obscured. We interpret this lack of local unit embayment as evidence that the emplacement and subsequent degradation of the first two highland units continued throughout much of the Noachian Period because of the high rate of surface impacts. The low-lying, basin-filling character of the Cimmeria 2 unit—relative to the Cimmeria 1 unit—suggests that the unit accumulated through the erosion of higher-standing units, likely as the result of fluvial, colluvial, and (or) lacustrine processes. Large-diameter impact craters are abundant in units Nhc_1 and Nhc_2, suggesting these are made up of significant amounts of impact-related ejecta and brecciated highland rocks (that is, Martian “regolith”). Local inclusions of volcanic rocks are possible, though lithologic and (or) depositional characteristics that definitively outline such components are sparse.

The occurrence of wrinkle ridges in the Cimmeria 2 unit indicates crustal shortening in both the east-west and north-south direction during the Middle to Late Noachian. Though younger units obscure the actual extent of unit Nhc_2 across the highland-lowland boundary scarp, it is likely that unit extended onto part of the proto-boundary plain. Local pitting and isolated knobs and mesas within unit Nhc_2 suggest it was modified by erosional deflation and (or) localized subsidence after emplacement during the Middle to Late Noachian.

Early Hesperian Epoch

The timing of events in this epoch is perhaps the most tightly controlled for the geologic units mapped within the Nepenthes Planum region owing to excellent exposure and well-constrained crater counts. We infer the existence of a depositional hiatus between the Cimmeria 2 and 3 units during the Late Noachian. Later, during the Late Noachian to Early Hesperian, the Cimmeria 3 unit ($HNhc_3$) was emplaced as irregularly shaped, isolated patches of bright, sloping, and hummocky surfaces on the lower reaches of the regional highland-lowland boundary scarp, particularly in impact crater basins and low-relief depressions bounded by the Cimmeria 2 unit. The unit also surrounds low-relief outliers of Cimmeria 1 unit. The Cimmeria 3 unit’s northern extent is obscured because of burial by younger units. The unit’s southern margins are commonly lobate in form. The occurrence of narrow, braided valleys and ridges (fig. 5) indicate the role of fluids in the emplacement history of the Cimmeria 3 unit. Outcrops in the southeastern map region contain rugged lobate margins and small depressions. These provide some evidence of their emplacement and modification through fluid processes, perhaps owing to eruption of lava or liquefied sediment followed by local subsidence and (or) collapse. The unit appears to pre-date all large (>16 km) diameter impact craters, with the exception of Ehden.

The Nepenthes vent and flow units (Htn_v and $Htnf_v$, respectively) dominate the central part of the map region and compose the areal bulk of Nepenthes Planum. The Nepenthes flow unit was emplaced as a series of overlapping lobes, evidenced by the lobate margin that forms the southern boundary, which overlies the Cimmeria 3 unit, as well as the occurrence of abundant lobes within the unit itself (fig. 6). The unit is interpreted to be composed of either erupted sheet lavas, fluidized sediments (mud flows), or perhaps a combination of both (Tanaka and others, 2003b). Source regions for the Nepenthes flow unit are likely to be the (large diameter) pitted cones and mounds that dot the region, as well as perhaps fissure-like troughs. Some flows are directly traceable to large-diameter pitted cones (Skinner and Tanaka, 2007) mapped as the Nepenthes vent unit, though others appear to emerge from the overall plains. The Nepenthes flow unit includes a characteristic rugged textural facies that we identify using a hachured pattern, whereas the remainder has a smoother surface. The rugged facies sometimes forms lobate margins but is more often associated with a lateral gradation to the smoother facies. The range of textures of the Nepenthes flow unit likely results from differing eruption characteristics and (or) post-eruption modification (for example, desiccation, deflation, and (or) aeolian scour and mantling).

The Nepenthes vent unit identifies constructional edifices formed through the eruption of pyroclasts (Brož and Hauber, 2013) or fluidized sediment (Skinner and Tanaka, 2007). Though each hypothesis offers a markedly different perspective on the geologic evolution of Nepenthes Planum—as well as the underlying tectonic environment—the determination of one hypothesis over another is complicated by the dominance of dust and a general lack of compositional signatures. Brož and Hauber (2013) favored a phreatomagmatic origin for the large pitted cones of Nepenthes Planum, which also occur in adjacent highland-lowland transitional zones to the west and northwest, based on their morphometric similarity to terrestrial tuff rings and cones. Skinner and Tanaka (2007), however, favored a mud volcano-like origin of the large pitted cones and small tholi based on their presumed occurrence within structurally annular compartments of the Utopia multi-ring impact basin (for example, McGill, 1989) as well as their extended distance from the large-scale Elysium volcanic center known to have been active during this time (Tanaka and others, 1992, 2014). The shape of the vents that make up the transitional vent unit changes across the map region; the eastern vents are small tholi and the western vents are large pitted cones with a central depression. Lobate materials appear to emanate from the latter in multiple instances. Small tholi that are located in the eastern map region are more commonly associated with wrinkle ridges, which Skinner and Tanaka (2007) cited as further evidence of a mud volcano-like genesis, resulting from subsurface pressures and the ascent and eruption of buoyant sediments. Brož and Hauber (2013) suggested that morphometry implicates an origin more akin to terrestrial lava coulees.

Large, north-south-oriented wrinkle ridges and scarps form the Hephaestus Rupēs, which occur in unit $\mathrm{Htn_v}$ of Nepenthes Planum. These ridge and scarp systems rarely extend into the Cimmeria 3 unit ($\mathrm{HNhc_3}$) to the south, suggesting that they formed within a discrete sequence of materials. Older, Cimmeria 1 unit ($\mathrm{Nhc_1}$) outcrops are the most dominant high-relief features in Nepenthes Planum and are erosional vestiges of geologic units associated with the cratered highlands. Well-defined ejecta blankets with rampart margins surround impact craters in this region. Past studies suggest that these crater-related landforms form as the result of the incorporation of subsurface water or ice into the impact-brecciated and ejected target materials, which form mobile, ground-hugging debris flows (for example, Barlow, 2006, 2010). Depth-diameter ratios of impact craters within this region are smaller than global averages (Boyce and others, 2005), implicating a lack of rheological strength in target materials such as may occur from weak (unconsolidated) rock sequences and (or) the presence of subsurface water and (or) ice during the Noachian and Hesperian.

Late Hesperian Epoch

The northern margin of Nepenthes Planum is defined by isolated and coalesced depressions of Amenthes Cavi, which are characterized by gently sloping margins and are often ringed by narrow, arcuate troughs. The Amenthes Cavi are filled with the Utopia 1 unit ($\mathrm{Hlu_1}$), which is characterized by a smooth surface. Unit $\mathrm{Hlu_1}$ is traceable to narrow troughs that bound Amenthes Cavi (fig. 8), which we interpret as evidence that these cavi-bounding linear shallow troughs were the source of unit $\mathrm{Hlu_1}$. Small, streamlined islands and shallow channels emanate from these narrow, arcuate troughs, suggesting that the material that occurs within—and apparently fills—the Amenthes Cavi had low viscosity (fig. 8). Given the association of arcuate fractures, channels and islands, and smooth cavi infill, we believe that the eruption of material to form the Utopia 1 unit ($\mathrm{Hlu_1}$) was contemporaneous with the fracturing of the Nepenthes flow unit ($\mathrm{Htn_f}$) formation of Amenthes Cavi through subsidence and (or) collapse. Evacuation of subsurface reservoirs of interstitial water presumably led to focused subsidence and marginal fracturing of the existing plains. A lack of lobes or channels within the Utopia 1 unit suggests that the material was made up of fine-grained clastic material emplaced largely by sheet flow. The Utopia 1 unit extends to the north 100 to 200 km and forms the first of two nearly horizontal lowland sequences within the map region.

Phedra, Tavua, Linpu, and Marbach craters are each located partly to wholly within Amenthes Cavi and are surrounded by ejecta that have been partly embayed by the Utopia 1 unit. The formation of Amenthes Cavi and eruption (or extrusion) of fluid material from the subsurface appears contemporaneous. Close association with large-diameter impact craters and their embayment by this younger unit raise the possibility that these impacts (separately or collectively) may have provided the triggering mechanism for the formation of parts of Amenthes Cavi and the contemporaneous eruption or extrusion of pressurized, fluidized subsurface material. The Utopia 1 unit embays and surrounds north-south ridges of the Nepenthes flow unit.

Amazonian Period

The materials that occur in the northern part of the map region are among the southernmost extension of materials that cover vast portions of the northern plains (Tanaka and others, 2005, 2014). Within the map region, this unit is mapped as the Utopia 2 unit ($\mathrm{AHlu_2}$) because of close spatial association and physical appearance with the Utopia 1 unit. The Utopia 2 unit was emplaced at the end of the Hesperian to the beginning of the Amazonian. A series of south-facing lobes define the Utopia 2 unit's southern margin. These lobes characteristically surround and embay tens-of-meters-high knobs and plateaus (fig. 2), which are mapped herein as outliers of the Nepenthes flow unit because their heights are consistent with those of larger, clearly identifiable outcrops of that unit to the south. The south-facing—and notably upslope—orientation of the Utopia 2 unit's southern margin implies fluid emplacement from the north. These features are similar in shape and orientation to others documented elsewhere along the northern plains margin

(Tanaka and others, 2005). Narrow, arcuate ridges that parallel the unit's lobate margin are common and are everywhere associated with sub-kilometer-diameter pitted cones. This ridge-cone pattern has been mapped and described as thumbprint terrain in several locations of the Martian northern plains (Tanaka and others, 2005).

References Cited

Barlow, N.G., 2006, Impact craters in the northern hemisphere of Mars—Layered ejecta and central pit characteristics: Meteoritics and Planetary Science, v. 41, no. 10, p. 1,425–1,436, doi: 10.1111/j.1945-5100.2006.tb00427.x.

Barlow, N.G., 2010, What we know about Mars from its impact craters: Geological Society of America Bulletin, v. 122, no. 5–6, p. 644–657, doi:10.1130/B30182.1.

Boyce, J.M., Mouginis-Mark, P., and Garbeil, H., 2005, Ancient oceans in the northern lowlands of Mars—Evidence from impact crater depth/diameter relationships: Journal of Geophysical Research—Planets, v. 109, no. E3, doi:10.1029/2004JE002328.

Bridges, J.C., Grady, M.M., Pillinger, C.T., and Sims, M.R., 1999, Landing site selection for the Beagle 2 mission to Mars: Meteoritics and Planetary Science, v. 34, no. 4 (supplement), p. A19.

Brož, P., and Hauber, E., 2013, Hydrovolcanic tuff rings and cones as indicators for phreatomagmatic explosive eruptions on Mars: Journal of Geophysical Research—Planets, v. 118, no. 8, p. 1,656–1,675, doi: 10.1012/jgre.20120.

Carr, M.H., and Head, J.W., III, 2003, Oceans on Mars—An assessment of the observational evidence and possible fate: Journal of Geophysical Research—Planets, v. 108, no. E5, p. 8–1 to 8–28, doi:10.1029/2002JE001963.

Christensen, P.R., Jakosky, B.M., Kieffer, H.H., Malin, M.C., McSween, H.Y., Nealson, K., Mehall, G.L., Silverman, S.H., Ferry, S., Caplinger, M., and Ravine, M., 2004, The Thermal Emission Imaging System (THEMIS) for the Mars 2001 Odyssey Mission: Space Science Reviews, v. 110, p. 85–130.

Clifford, S.M., and Parker, T.J., 2001, The evolution of the Martian hydrosphere—Implications for the fate of a primordial ocean and the current state of the northern plains: Icarus, v. 154, no. 1, p. 40–79, doi:10.1006/icar.2001.6671.

Federal Geographic Data Committee [prepared for the Federal Geographic Data Committee by the U.S. Geological Survey], 2006, FGDC Digital cartographic standard for geologic map symbolization: Reston, Va., Federal Geographic Data Committee Document Number FGDC–STD–013–2006, 290 p., 2 plates.

Frey, H.V., and Schultz, R.A., 1990, Speculations on the origin and evolution of the Utopia-Elysium lowlands of Mars: Journal of Geophysical Research—Solid Earth, v. 95, no. B9, p. 14,203–14,213, doi:10.1029/JB095iB09p14203.

Ghatan, G.L., and Zimbelman, J.R., 2006, Paucity of candidate coastal constructional landforms along proposed shorelines on Mars—Implications for a northern lowlands-filling ocean: Icarus, v. 185, no. 1, p. 171–196, doi:10.1016/j.icarus.2006.06.007.

Golombek, M.P., Cook, R.A., Moore, H.J., and Parker, T.J., 1997, Selection of the Mars Pathfinder landing site: Journal of Geophysical Research—Planets, v. 102, no. E2, p. 3,967–3,988, doi:10.1029/96JE03318.

Greeley, R., and Batson, R.M., eds., 1990, Planetary mapping: New York, NY, Cambridge University Press, 296 p.

Greeley, Ronald, and Guest, J.E., 1987, Geologic map of the eastern equatorial region of Mars: U.S. Geological Survey Geologic Investigations Series Map I–1802–B, scale 1:15,000,000.

Hansen, V.L., 2000, Geologic mapping of tectonic planets: Earth and Planetary Science Letters, v. 176, no. 3–4, p. 527–542, doi:10.1016/S0012-821X(00)00017-0.

Head, J.W., III, Kreslavsky, Mikhail, Hiesinger, Harald, Ivanov, Mikhail, Pratt, Stephen, and Seibert, Nicole, 1998, Oceans in the past history of Mars—Tests for their presence using Mars Orbiter Laser Altimeter (MOLA) data: Geophysical Research Letters, v. 25, no. 24, p. 4,401–4,404, doi:10.1029/1998GL900116.

Hiller, K.H., 1979, Geologic map of the Amenthes quadrangle of Mars: U.S. Geological Survey Miscellaneous Investigations Map I-1110, scale 1:5,000,000.

Ivanov, M.A., Hiesinger, H., Erkeling, G., and Reiss, D., 2014, Mud volcanism and morphology of impact craters in Utopia Planitia on Mars—Evidence for the ancient ocean: Icarus, v. 228, p. 121–140, doi:10.1016/j.icarus.2013.09.018.

Kopf, A.J., 2002, Significance of mud volcanism: Reviews of Geophysics, v. 40, no. 2, p. 2-1 to 2-52, doi:10.1029/2000RG000093.

Kreslavsky, M.A., and Head, J.W., III, 2000, Kilometer-scale roughness of Mars—Results from MOLA data analysis: Journal of Geophysical Research—Planets, v. 105, no. E11, p. 26,695–26,711, doi:10.1029/2000JE001259.

Kreslavsky, M.A., and Head, J.W., 2002, Fate of outflow channel effluents in the northern lowlands of Mars—The Vastitas Borealis Formation as a sublimation residue from frozen ponded bodies of water: Journal of Geophysical Research—Planets, v. 107, no. E12, p. 4-1 to 4-25, doi:10.1029/2001JE001831.

Masursky, Harold, and Crabill, N.L., 1981, Viking site selection and certification: NASA Special Paper, no. 429.

McGill, G.E., 1989, Buried topography of Utopia, Mars—Persistence of a giant impact depression: Journal of Geophysical Research—Solid Earth, v. 94, no. B3, p. 2,753–2,759.

Nimmo, Francis, and Tanaka, Ken, 2005, Early crustal evolution of Mars: Annual Review of Earth and Planetary Sciences, v. 33, p. 133–161, doi:10.1146/annurev.earth.33.092203.122637.

Parker, T.J., Gorsline, D.S., Saunders, R.S., Pieri, D.C., and Schneeberger, D.M., 1993, Coastal geomorphology of the Martian northern plains: Journal of Geophysical Research—Planets, v. 98, no. E6, p. 11,061–11,078, doi:10.1029/93JE00618.

Platz, Thomas, Michael, Gregory, Tanaka, K.L., Skinner, J.A., Jr., and Fortezzo, C.M., 2013, Crater-based dating of geological units on Mars—Methods and application for the new global geological map: Icarus, v. 225, no. 1, p. 806–827, doi:10.1016/j.icarus.2013.04.021.

Salvatore, A., ed., 1994, International stratigraphic guide—A guide to stratigraphic classification, terminology, and procedure (2d ed.): Boulder, Colo., The Geological Society of America, 214 p.

Scott, D.H., and Carr, M.H., 1978, Geologic map of Mars: U.S. Geological Survey Miscellaneous Investigations Map I-1083, scale 1:25,000,000.

Skinner, J.A., Jr., and Tanaka, K.L., 2007, Evidence for and implications of sedimentary diapirism and mud volcanism in the southern Utopia highland-lowland boundary plain, Mars: Icarus, v. 186, no. 1, p. 41–59, doi:10.1016/j.icarus.2006.08.013.

Skinner, J.A., Jr., and Mazzini, Adriano, 2009, Martian mud volcanism—Terrestrial analogs and implications for formational scenarios: Marine and Petroleum Geology, v. 26, no. 9, p. 1,866–1,878, doi:10.1016/j.marpetgeo.2009.02.006.

Smith, D.E., Zuber, M.T., Frey, H.V., and 21 others, 2001, Mars Orbiter Laser Altimeter—Experiment summary after the first year of global mapping of Mars: Journal of Geophysical Research—Planets, v. 106, no. E10, p. 23,689–23,722, doi:10.1029/2000JE001364.

Tanaka, K.L., 1986, The Stratigraphy of Mars, *in* Proceedings of the seventeenth Lunar and Planetary Science Conference, Part 1: Journal of Geophysical Research—Solid Earth, v. 91, no. B13, p. E139–158.

Tanaka, K.L., Carr, M.H., Skinner, J.A., Gilmore, M.S., and Hare, T.M., 2003b, Geology of the MER 2003 “Elysium” candidate landing site in southeastern Utopia Planitia, Mars: Journal of Geophysical Research—Planets, v. 108, no. E12, doi:10.1029/2003JE002054.

Tanaka, K.L., Chapman, M.G., and Scott, D.H., 1992, Geologic map of the Elysium region of Mars: U.S. Geological Survey Miscellaneous Investigations Map I-2147, scale 1:5,000,000.

Tanaka, K.L., Skinner, J.A., Jr., Dohm, J.M., and 6 others, 2014, Geologic map of Mars: U.S. Geological Survey Scientific Investigations Map 3292, scale 1:20,000,000.

Tanaka, K. L., Skinner, J. A., Jr., and Hare, T. M., 2005, Geologic map of the northern plains of Mars: U.S. Geological Survey Scientific Investigations Map 2888, scale 1:15,000,000.

Tanaka, K.L., Skinner, J.A., Jr., Hare, T.M., Joyal, Taylor, and Wenker, Alisa, 2003a, Resurfacing history of the northern plains of Mars based on geologic mapping of Mars Global Surveyor data: Journal of Geophysical Research—Planets, v. 108, no. E4, doi:10.1029/2002JE001908.

Werner, S.C., and Tanaka, K.L., 2011, Redefinition of the crater-density and absolute-age boundaries for the chronostratigraphic systems of Mars: Icarus, v. 215, no. 2, p. 603–607, doi:10.1016/j.icarus.2011.07.024.